RSC Advances

PAPER

Cite this: *RSC Adv.*, 2022, **12**, 13319

Selective hydroconversion of coconut oil-derived lauric acid to alcohol and aliphatic alkane over MoO_x-modified Ru catalysts under mild conditions†

Rodiansono, *[ab] Heny Puspita Dewi,[ab] Kamilia Mustikasari,[a] Maria Dewi Astuti,[a] Sadang Husain[c] and Sutomo[d]

Molybdenum oxide-modified ruthenium on titanium oxide (Ru–(*y*)MoO_x/TiO_2; *y* is the loading amount of Mo) catalysts show high activity for the hydroconversion of carboxylic acids to the corresponding alcohols (fatty alcohols) and aliphatic alkanes (biofuels) in 2-propanol/water (4.0/1.0 v/v) solvent in a batch reactor under mild reaction conditions. Among the Ru–(*y*)MoO_x/TiO_2 catalysts tested, the Ru–(0.026)MoO_x/TiO_2 (Mo loading amount of 0.026 mmol g^{-1}) catalyst shows the highest yield of aliphatic *n*-alkanes from hydroconversion of coconut oil derived lauric acid and various aliphatic fatty acid C6–C18 precursors at 170–230 °C, 30–40 bar for 7–20 h. Over Ru–(0.026)MoO_x/TiO_2, as the best catalyst, the hydroconversion of lauric acid at lower reaction temperatures (130 ≥ *T* ≤ 150 °C) produced dodecane-1-ol and dodecyl dodecanoate as the result of further esterification of lauric acid and the corresponding alcohols. An increase in reaction temperature up to 230 °C significantly enhanced the degree of hydrodeoxygenation of lauric acid and produced *n*-dodecane with maximum yield (up to 80%) at 230 °C, H_2 40 bar for 7 h. Notably, the reusability of the Ru–(0.026)MoO_x/TiO_2 catalyst is slightly limited by the aggregation of Ru nanoparticles and the collapse of the catalyst structure.

Received 1st April 2022
Accepted 26th April 2022

DOI: 10.1039/d2ra02103j

rsc.li/rsc-advances

Introduction

The catalytic hydroconversion of fatty acids and their esters into fatty alcohols and aliphatic alkanes is receiving increased attention in the context of upgrading of bio-based feedstocks by using heterogeneous mono- or bi-metallic catalysts.[1–4] Both fatty alcohols and aliphatic alkanes are basic building blocks in organic synthesis, living organisms, energy, fuels, surfactants, lubricants, plasticizers, coatings, polymers, and the materials industry.[5,6] The catalytic hydroconversion of fatty acids can be classified into three reactions: hydrodeoxygenation (HDO), hydrodecarbonylation (HDCO), and hydrodecarboxylation ($HDCO_2$), and a number of comprehensive reviews have been reported in the last decade.[7–12] HDCO and $HDCO_2$ yield hydrocarbons with one carbon atom less than the fatty acid precursor, while HDO gives hydrocarbons with the same chain length as the starting compounds.[13] Among these hydroconversion approaches, HDO, producing hydrocarbons without C–C bond cleavage of fatty acids, is more atom-efficient than the other methods (HDCO and $HDCO_2$) with C–C bond cleavage of the fatty acids. Moreover, the reaction rate of HDCO or $HDCO_2$ is slow and needs to be carried out at higher reaction temperatures.[14]

The development of effective heterogeneous catalyst systems (in the form of supported reduced or sulfided metals or bimetallic) for the hydroconversion of fatty acids has been long-standing industrial target by researchers.[15–18] The literature shows that heterogeneous supported platinum group metals (PGM) (*e.g.*, Pt, Pd, Rh, Ru, Ni) catalysts showed high selectivity toward HDCO or $HDCO_2$ rather than HDO products even under H_2 atmosphere.[19–23] To improve the HDO activity rather than HDCO and $HDCO_2$ of fatty acids, the modification of those PGM-based catalysts is necessary, *i.e.*, the addition of more electropositive metals[24,25] or the use of oxide supports that strongly interact with the active metals,[26–28] or direct modification with the metal oxide species.[29] The addition of second metals (*e.g.*, Sn and B) to Ru enhanced the dispersion of Ru and improved the electron density of Ru. The change of electron

[a]*Department of Chemistry, Faculty of Mathematics and Natural Sciences, Lambung Mangkurat University, Jl. A. Yani Km 36.0, Banjarbaru, South Kalimantan, Indonesia*
[b]*Catalysis for Sustainable Energy and Environment (CATSuRe), Lambung Mangkurat University, Indonesia. E-mail: rodiansono@ulm.ac.id; Fax: +625114773112; Tel: +625114773112*
[c]*Department of Physics, Faculty of Mathematics and Natural Sciences, Lambung Mangkurat University, Indonesia*
[d]*Department of Pharmacy, Faculty of Mathematics and Natural Sciences, Lambung Mangkurat University, Indonesia*

† Electronic supplementary information (ESI) available: Characterisation of catalyst materials: physico-chemical properties, XRD, NH_3-TPD, pyridine adsorption, TEM images. See https://doi.org/10.1039/d2ra02103j

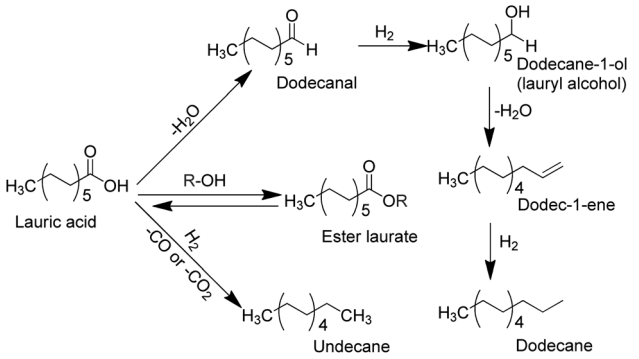

Scheme 1 Possible reaction pathways for the hydroconversion of lauric acid to alcohols and aliphatic alkanes.

density Ru enhanced the affinity of Ru towards C=O bond of fatty acids which facilitated the reaction hydrogenation.[30–32] Several bimetallic or alloy-based catalysts (*e.g.*, Pd–M (M = Cu, Co, Ni),[33] Ni–Sn/TiO_2,[34] Pd–Nb_2O_5,[35] Ru–Sn,[31] Rh–Sn,[32] and Pd–Sn/C,[36]) have shown superior performance for the selective hydrogenation of fatty acids compared with their single metal counterpart. Luo *et al.* reported the hydrogenation of coconut oil to fatty alcohols using nanocluster Ru_3Sn_7/SiO_2 catalysts at 240 °C, 40 bar. They claimed that Ru_3Sn_7 and SnO_x were active species in the bimetallic Ru–Sn catalyst as indicated by the conversion and product selectivity, and computational modelling calculation.[37,38] In the case of direct modification of PGM with metal oxides, oxophilic metal oxides (*e.g.*, ReO_x, MoO_x, and WO_x)-modified PGM-based catalysts showed excellent performance for the catalytic HDO of biomass-derived oxygenates into chemicals and fuels.[39–45] The presence of oxophilic metal oxides played the bifunctional catalytic roles, whereas the metal sites can catalyse the hydrogen uptake, dissociation, and spill-over onto the metal-oxide in vicinity.[46,47] It was believed that H_2 spill-over facilitated the partial reduction of metal-oxide species and generated a new site active in interface of metal–metal oxide. Moreover, the reduced metal–oxide species can act as Lewis acid sites for the C–O bond cracking *via* dehydration reaction.[29,48–51]

Lauric acid is one of typical bio-based aliphatic fatty acids with medium carbon length (C12) that mainly constituent of coconut oil or palm kernel oil (~50%),[52,53] which can be transformed into lauryl alcohol (dodecane-1-ol) and aliphatic alkanes (*e.g.*, *n*-dodecane or undecane). We have developed bimetallic catalysts (*e.g.*, bimetallic Ni–Sn/TiO_2, Pd–Fe/TiO_2, Pd–Sn/C and Ru–Fe/TiO_2 catalysts) and showed high catalytic performances in the hydrogenation of typical biomass-derived levulinic acid to γ-valerolactone,[54–56] lauric acid to dodecane-1-ol,[34,57] and stearic acid to octadecanol.[36] In the present paper, we describe our studies on the hydroconversion of lauric acid into lauryl alcohol using molybdenum oxide-modified ruthenium supported on titanium oxide (denoted as Ru–(y)MoO_x/TiO_2; y = loading amount of Mo, mmol g^{-1}) catalysts. The addition of Mo (~0.026 mmol; Mo/Ru = 0.5) to Ru/TiO_2 catalyst (denoted as Ru–(0.026)MoO_x/TiO_2) greatly improved the hydrodeoxygenation of lauric acid and produced *n*-dodecane (~72% yield) at 190 °C, 40 bar H_2, and a reaction time of 7 h. An increase in reaction temperature to 200–230 °C significantly enhanced the degree of hydrodeoxygenation of lauric acid and yield of *n*-dodecane reached to maximum (80%) (Scheme 1). Therefore, the effect of solvent used, reaction temperature, initial H_2 pressure, and reaction time on the yields of desired products during the hydroconversion of lauric acid are discussed systematically.

Results and discussion

Catalytic reactions

Screening of solvents. In the first set experiments, the catalytic hydroconversions of lauric acid over Ru–(0.026)MoO_x/TiO_2 catalyst (Mo = 0.026 mmol) were performed in various solvents and the results are summarised in Table 1. In alcoholic solvents, such as methanol, ethanol, and 1-propanol, the yields of dodecane-1-ol and ester laurate were 17–43% and 49–59%, respectively (entries 1–3). By using 2-propanol, the highest yield of dodecane-1-ol (87%) was obtained with a small amount of dodecyl dodecanoate (4%) as the side product of esterification of lauric acid and dodecane-1-ol at 91% conversion of lauric acid (entry 4). Moreover, further hydrodeoxygenation of lauric acid or lauryl alcohol to produce aliphatic *n*-alkanes is inhibited in alcoholic solvents under the current reaction conditions.

Interestingly, a remarkable difference was observed in H_2O, the products were distributed to dodecane-1-ol (32% yield) and *n*-dodecane (17% yield) at 52% conversion of lauric acid (entry 5), indicating that the hydrodeoxygenation lauric acid to aliphatic alkanes occurred in H_2O. The importance of H_2O media in the catalytic hydrothermal deoxygenation (330 °C) of fatty acids had been noticed to improve the yield of alipathic alkanes in the presence of supported PGM catalysts.[2,58,59] Moreover, under hydrothermal conditions, the presence of molecular water promoted the $HDCO_2$ reaction generating less one carbon of aliphatic alkanes and CO_2 as side product.[60] In our reaction system, the presence of external H_2 prevent the decarboxylation reaction and allow the hydroconversion of lauric acid under milder reaction conditions. However, the dodecyl dodecanoate (3%) product of esterification between lauric acid and dodecan-1-ol was obviously observed in H_2O. This results let us to further investigation the effect of solvent to enhance conversion and yield, particularly, in alcohol and H_2O mixture solvents. In methanol/H_2O (4.0 : 1.0 volume ratio), the conversion of lauric acid was 84% and the yield of dodecane-1-ol significantly increased by approximately three times (43%) while yields of dodecane and methyl laurate were 11% and 30%, respectively (entry 6). The catalytic reactions in ethanol/H_2O, 1-propanol/H_2O, and 2-propanol/H_2O solvent mixtures significantly enhanced the hydrodeoxygenation of lauric acid reaction as indicated by the increase of *n*-dodecane or the decrease of ester laurate yields (entries 7–9). It can be seen that catalytic reactions in 2-propanol or 2-propanol/H_2O are superior which can be attributed to the relatively higher solubility degree of lauric acid than that other solvents.[61–63] The synergistic effect between intrinsic properties of solvent (*e.g.*, dielectric constant and donation number) and the Brønsted acidity of catalysts

Table 1 Results of solvent screening for the selective hydroconversion of lauric acid over Ru–(0.026)MoO_x/TiO_2 catalyst (Mo = 0.026 mmol)[a]

Entry	Solvent[b]	Dielectric constant of solvent (ε)	Donor number (DN)	Conversion[c] (%)	Yield[c](%)		
					Dodecane-1-ol	*n*-Dodecane	Esters
1	Methanol	32.7	19.0	74	17	0	57[d]
2	Ethanol	24.5	19.2	82	22	0	59[d]
3	1-Propanol	21.8	19.8	92	43	0	49[d]
4	2-Propanol	19.9	21.1	91	87	0	4[e]
5	H_2O	80.1	18.0	52	32	17	3[e]
6	Methanol/H_2O (4.0 : 1.0 v/v)	—	—	84	43	11	30[d]
7	Ethanol/H_2O (4.0 : 1.0 v/v)	—	—	95	59	12	24[d]
8	1-Propanol/H_2O (4.0 : 1.0 v/v)	—	—	>99	53	20	26[d]
9	2-Propanol/H_2O (4.0 : 1.0 v/v)	—	—	>99	61	38	<0.1[e]

[a] Reaction conditions: catalyst, 0.065 g; lauric acid, 3.2 mmol; solvent, 5 mL, 170 °C; H_2 40 bar, 7 h. [b] The value in the parenthesis is volume ratio of solvent. [c] Conversion and yield were determined by GC using an internal standard technique. [d] Methyl, ethyl, and propyl laurate are included as the esterification lauric acid with the solvent as identified by using GC-MS analysis. [e] Dodecyl dodecanoate is included as the esterification of lauric acid and dodecane-1-ol. The carbon balance was 93–96% for all the catalyst.

during hydroconversion of lauric acid to lauryl alcohol and alkane might pronounce the stabilization of the acidic proton relative to the protonated transition states, leading to accelerated reaction rates for these acid-catalyzed biomass conversion reactions.[64,65] The catalytic reactions in various solvents other than alcohols and H_2O such as 1,4-dioxane, tetrahydrofuran (THF) and its mixture with H_2O were carried, however the yield of targeted products were insufficient under the reaction conditions.[57] Moreover, the highest yield (38%) of *n*-dodecane was achieved in 2-propanol/H_2O without the formation of ester laurate at >99% conversion of lauric acid (entry 9). Therefore, we conclude that the optimised solvent system for the hydroconversion of lauric acid to dodecane-1-ol or *n*-dodecane using Ru–MoO_x catalysts was in 2-propanol/H_2O (4.0 : 1.0 volume ratio).

Screening of catalysts. We synthesised various molybdenum oxide modified-ruthenium catalysts (the physicochemical properties of the synthesised Ru–(y)MoO_x/TiO_2 catalysts are summarised in Table S1,† XRD patterns (Fig. S1†), and typical TEM images of Ru−(0.026)MoO_x/TiO_2 and Ru–(0.048)MoO_x/TiO_2 are shown in Fig. S2 and S3, in the ESI†) and tested for the hydroconversion of lauric acid at 170 °C, 40 bar H_2 and 5 h and the results are summarised in Table 2. At the first, we prepared Ru/TiO_2 (Ru = 5 wt%) catalyst and tested for the hydroconversion of lauric acid. A 73% conversion of lauric acid was obtained and the products were dodecane-1-ol (65%), *n*-dodecane (4%), and ester (4%) (entry 1). After introducing a 0.026 mmol of Mo (Mo/Ru = 0.5) to Ru/TiO_2 catalyst (denoted as Ru–(0.026)MoO_x/TiO_2(A) A = anatase), a remarkably enhanced yield of *n*-dodecane to 38% was obtained at >99% conversion of lauric acid, whereas the yield of dodecane-1-ol was nearly constant (61%) (entry 2). The differences in the obtained reaction products from the catalytic reaction of lauric acid over Ru/TiO_2 and Ru–(0.026)MoO_x/TiO_2 catalysts were clearly observed, suggesting that the presence of Mo in the Ru–(0.026)MoO_x/TiO_2 catalyst plays a prominent role in the hydrogenation of lauric acid to dodecane-1-ol and *n*-dodecane. In the case of Ru–(0.026)MoO_x/TiO_2(R)(R = rutile) catalyst, the products were 82% dodecane-1-ol, 10% *n*-dodecane, and 8% others at >99% conversion of lauric acid under the same reaction

Table 2 Results of catalyst screening for selective hydroconversion of dodecanoic acid into dodecane-1-ol

Entry	Catalyst[a]	Conversion[b] (%)	Yield[b](%)		
			Dodecane-1-ol	*n*-Dodecane	Others[c]
1	Ru/TiO_2	73	65	4	4
2	Ru–(0.026)MoO_x/TiO_2(A)	>99	61	38	Trace
3	Ru–(0.026)MoO_x/TiO_2(R)	>99	82	10	8
4[d]	Ru/TiO_2 + $(NH_4)_6Mo_7O_{24}\cdot 4H_2O$	>99	45	9	46
5[d]	Ru/TiO_2 + MoO_x	97	42	12	43
6[e]	Ru@MoO_x	98	59	7	32

[a] The amount of Mo was arround 0.025 mmol (1 wt% to Ru metal based on the amount of precursor). Reaction conditions: catalyst, 0.065 g; lauric acid, 3.2 mmol; solvent, 2-propanol: H_2O, 5 ml (4.0 : 1.0 volume ratio), 170 °C; H_2 40 bar, 7 h. [b] Conversion and yield were determined by GC using an internal standard technique. [c] Others include dodecyl dodecanoate as the esterification of lauric acid and dodecane-1-ol and products with smaller carbon number according to GC-MS profiles. [d] The catalysts were prepared using physical mixing at room temperature, dried at 110 °C for 5 h, followed by reduction with H_2 at 500 °C for 3 h. [e] The catalyst was prepared using one-pot hydrothermal of $RuCl_3$ and $(NH_4)_6Mo_7O_{24}\cdot 4H_2O$ mixture solutions at 150 °C for 24 h, followed by reduction with H_2 at 500 °C for 3 h. The carbon balance was 93–96% for all the catalyst.

conditions (entry 3). Therefore, further discussion on the effect of various Mo loading amounts on the conversion of lauric acid and the yields of dodecane-1-ol and *n*-dodecane will be discussed later in this paper. Since remarkable enhancement of lauric acid conversion and *n*-dodecane yield were obtained and to confirm the role of Mo additions, physical mixtures of Ru/TiO_2 and $(NH_4)_6Mo_7O_{24}\cdot 4H_2O$ or MoO_x catalysts (the loading amount of Mo was 0.025 mmol to keep the Mo/Ru molar ratio of approximately 0.5) were prepared and also used for the reaction. Over Ru/TiO_2 + $(NH_4)_6Mo_7O_{24}\cdot 4H_2O$, the conversion of lauric acid was >99 and the products were distributed to dodecane-1-ol (45%), *n*-dodecane (9%), and others (46%) (entry 4).

A relatively high yield of others (46%) (mainly contain dodecyl dodecanoate ester and others smaller carbon number of compounds) was obtained, suggesting that $(NH_4)_6Mo_7O_{24}\cdot 4H_2O$ (may be as Mo^{+6}) promoted the further reaction of alcohol and acid to form ester or decomposition of reactant/product into small molecule (entry 4). The Ru/TiO_2 + MoO_x catalyst was also active for the hydroconversion of lauric acid (97% conversion) and the products were distributed to dodecane-1-ol (42%), *n*-dodecane (12%), and others (43%) (entry 5). Moreover, Ru@MoO_x exhibited high conversion of lauric acid (98%) towards dodecane-1-ol as the main product (59%), while yields of *n*-dodecane and others were 7% and 32% (respectively) (entry 6). The yield of others obtained over this catalyst was smaller than that of the Ru/TiO_2 + $(NH_4)_6Mo_7O_{24}\cdot 4H_2O$ system. These results suggested that the presence of both Mo^{6+} and MoO_x showed notable promotion effect on the dodecane-1-ol and *n*-dodecane formation, which are literally different between with and without the addition of $(NH_4)_6Mo_7O_{24}\cdot 4H_2O$ or MoO_x powder. The high conversion of lauric acid can be attributed to the presence of Mo, which can interact strongly with water solvent to contribute to construct and maintain the active species of Mo–OH in the form of H_x-MoO_x. The total acidity (obtained from NH_3 temperature programmed desorption (NH_3-TPD) and pyridine adsorption confirmed the presence of Brønsted and Lewis acid sites (Tabel S1 and Fig. S4 and S5, in the ESI†). The H_xMoO_x species acts as the Brønsted sites and helps to stabilise the transition state *via* hydrogen bonding during the hydrogenolysis of tetrahydrofurfuryl alcohol to 1,5-pentanediol.[50] It has been reported that MoO_3 is one of the reducible oxide supports which is commonly used as a co-promotor to enhance the activity and selectivity of PGM in the hydrogenation of carboxylic acids. The activity increase caused by reducible oxide supports is attributed to oxygen interaction with metallic ions of the support and/or oxygen vacancies on the metal-support interface. These electrophilic groups promote hydrogenation of the carboxylic acid by interacting with the carbonyl oxygen and weakening the C=O bond.[66,67] Alternatively, the MoO_x species in the Ru–MoO_x/TiO_2 would be partially reduced to MoO_x ($0 \le x \le 3$) by activated hydrogen atoms migrated *via* spill over from Ru nanoparticles considering the readily dissociation of H_2 on Ru.[67–69] Shimizu and co-workers reported that the presence of MoO_x co-loaded Pt/TiO_2 catalyst showed higher selectivity to CH_3OH from CO_2 hydrogenation than that without the presence of MoO_x.[70]

Ru–MoO_x on various supports. Six types of supports (γ-Al_2O_3, active carbon (C), C–TiO_2, ZrO_2, and ZnO) were employed for the preparation of the supported Ru–MoO_x catalysts using a procedure similar to that used for the synthesis of Ru–MoO_x/TiO_2 (XRD patterns of Ru–MoO_x on various supports are shown in Fig. S6, in the ESI†). Ru–MoO_x supported on carbon (Ru–MoO_x/C) gave high yield of dodecan-1-ol (89%) at >99% conversion of lauric acid with small amount of *n*-dodecane yield (9%) (entry 1). These results are very consistent with previous reports of Takeda *et al.* that the presence of MoO_x species in Ru–MoO_x/C catalyst enhanced the selectivity of diols or primary alcohols from aqueous phase hydrogenation of lactic acid and various low carbon number of carboxylic acids.[71] Interestingly, Ru–MoO_x supported on carbon doped-titanium oxide (Ru–MoO_x/C–TiO_2), which was obtained from one-pot hydrothermal of $TiCl_4$ and glucose solutions at 150 °C for 24 h as reported previously (XRD patterns are shown in Fig. S7, in the ESI†),[72,73] gave dodecane-1-ol (68%), *n*-dodecane (23%), and others (8%) (entry 2). Ru–MoO_x supported on γ-Al_2O_3 and SiO_2 catalysts showed lower lauric acid conversion (72–80%) and produced dodecane-

Table 3 Results of selective hydroconversion of dodecanoic acid into dodecane-1-ol over Ru–MoO_x catalysts on various supports and PGM metal based catalysts

			Yield[b](%)			
Entry	Catalyst[a]	Conversion[b] (%)	Dodecane-1-ol	*n*-Dodecane	Others[c]	Ref.
1	Ru–MoO_x/C	>99	89	9	2	This work
2	Ru–MoO_x/C–TiO_2	99	68	23	8	This work
3	Ru–MoO_x/γ-Al_2O_3	80	63	10	7	This work
4	Ru–MoO_x/SiO_2	72	52	12	8	This work
5	Ru–MoO_x/ZrO_2	55	53	0	2	This work
6[d]	Ru–MoO_x/TiO_2	>99	20	80	0	This work
7[e]	Pt–MoO_x/TiO_2	>99	2	86	8	13
8[e]	Pt/Nb_2O_5	>99	7	60	21	74
9[f]	Ni_3Sn_2/TiO_2	85	80	3	2	34

[a] The amount of Mo was arround 0.025 mmol (based on the precursor). Reaction conditions: catalyst, 0.065 g; lauric acid, 3.2 mmol; solvent, 2-propanol: H_2O, 5 mL (4.0 : 1.0 volume ratio), 170 °C; H_2 40 bar, 7 h. [b] Conversion and yield were determined by GC using an internal standard technique. [c] Dodecyl dodecanoate is included as the esterification of lauric acid and dodecane-1-ol. The carbon balance was 93–96% for all the catalysts. [d] At 230 °C, 40 bar, 7 h. [e] At 180 °C, 80 bar, 4 h. [f] At 160 °C, 30 bar 20 h.

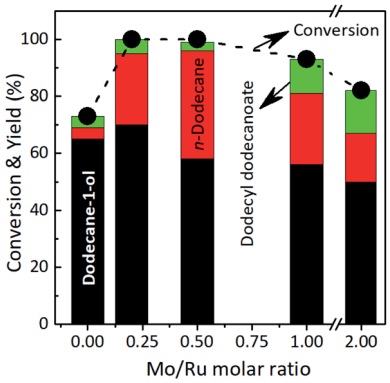

Fig. 1 Results of product distribution (yield) from selective hydroconversion of lauric acid using Ru–MoO_x/TiO_2 catalysts with different Mo loading amounts. Reaction conditions: catalyst, 0.065 g; lauric acid, 3.2 mmol; solvent, 2-propanol: H_2O, 5 mL (4.0 : 1.0 volume ratio); H_2 40 bar, 170 °C, 7 h.

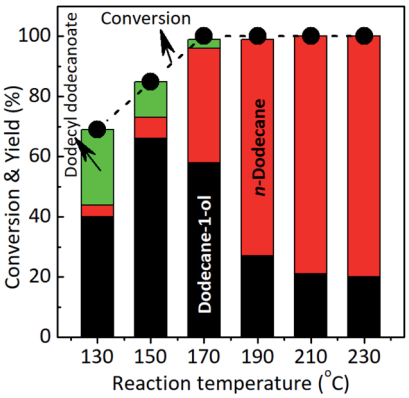

Fig. 3 Effect of reaction temperature on the conversion and yield in the hydroconversion of lauric acid over Ru–(0.026)MoO_x/TiO_2 catalyst. Reaction conditions: catalyst, 0.065 g; lauric acid, 3.2 mmol; solvent, 2-propanol: H_2O, 5.0 mL (4.0 : 1.0 volume ratio); H_2 40 bar, 7 h.

1ol (52–63%), *n*-dodecane (10–12%), and others (~8%) (entries 3–4). Moreover, Ru–MoO_x/ZrO_2 catalyst produced only dodecane-1-ol (53%) without the formation of *n*-dodecane under the same reaction conditions (entry 5). The effectiveness of TiO_2 or C–TiO_2 supported Ru–MoO_x catalysts in the hydroconversion of lauric acid to alcohol and alkane were superior than the other supported catalysts. These results can be attributed to the synergistic action between MoO_x species and reducible support (*e.g.* TiO_2). Intimate interaction between Ru–MoO_x and support with different energy of electron affinity may affect to the electron state of Ru.[13,74] In addition, our best result of alkane yield was obtained using Ru–(0.026)MoO_x/TiO_2 catalyst at 230 oC, 40 bar 7 h (80% in yield) (entry 6), which comparable to the results obtained by using Pt–MoO_x/C (entries 7 and 8)[13] and much higher than that of Ni_3Sn_2/TiO_2 catalyst (entry 9)[35] (Table 3).

Effect of Mo loading amounts (Mo/Ru molar ratio). To obtain the insight into the role of Mo modified on the Ru-based catalysts, four types of Ru–(*y*)MoO_x/TiO_2 (*y* = loading amount of Mo, *ca.* 0.000; 0.011; 0.025; 0.045; and 0.098 mmol) catalysts were prepared (the XRD patterns are shown in Fig. S8, in the ESI†) and tested for the selective hydroconversion of lauric acid to dodecane-1-ol and *n*-dodecane and the results are shown in Fig. 1. By using Ru/TiO_2 (Mo = 0.0 mmol), the conversion of lauric acid was 73% with yields of dodecane-1-ol, *n*-dodecane, and dodecyl dodecanoate were 65%, 4% and 4%, respectively (entry 1, Table 1). After a 0.011 mmol Mo was introduced to form Ru–MoO_x/TiO_2 (Mo = 0.011 mmol); Mo/Ru = 1/4.5) catalyst, the conversion of lauric acid dramatically increased to 100% and yields of dodecane-1-ol, *n*-dodecane, and dodecyl dodecanoate were 70%, 25%, and 5%, respectively. A slight increase of *n*-dodecane yield (38%) was obtained over Ru–MoO_x/TiO_2 (Mo = 0.026 mmol; Mo/Ru = 1/2.0) catalyst at completed conversion of lauric acid. The conversion of lauric acid slightly decreased (93%), whereas the yields of dodecane-1-ol, *n*-dodecane, dodecyl dodecanoate were 56%, 25%, and 12%, respectively, when Ru–Mo/TiO_2 (Mo = 0.049; Mo/Ru = 1/1.0)

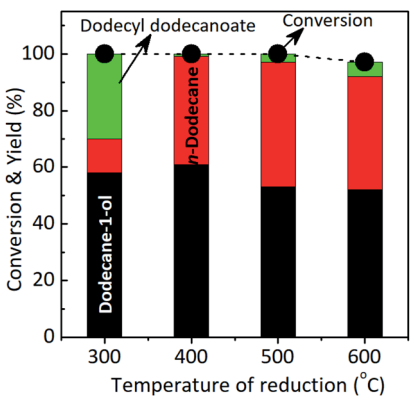

Fig. 2 Results of product distribution (yield) from selective hydroconversion of lauric acid using Ru–(0.026)MoOx/TiO_2 catalyst with different Mo loading amounts. Reaction conditions: catalyst, 0.065 g; lauric acid, 3.2 mmoL; solvent, 2-propanol: H_2O, 5 ml (4.0 : 1.0 volume ratio); H_2 40 bar, 170 °C, 7 h.

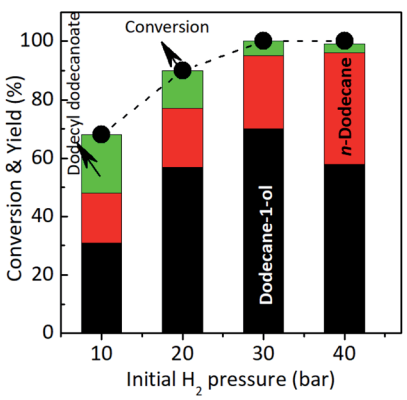

Fig. 4 Effect of initial H_2 pressure on the conversion and yield in the hydroconversion of lauric acid over Ru–(0.026)MoO_x/TiO_2 catalyst. Reaction conditions: catalyst, 0.065 g; lauric acid, 3.2 mmol; solvent, 2-propanol: H_2O, 5.0 ml (4.0 : 1.0 volume ratio); 170 °C, 7 h.

catalyst was used. Further increase the loading of Mo (*ca.* 0.098 mmol; Mo/Ru = 2.0/1.0), both conversion of lauric acid and yields of dodecane-1-ol, and *n*-dodecane significantly decreased, whereas yield dodecyl dodecanoate slightly increased to 15%. To understand the beneficiary effect of Mo species on the Ru/C system, we examined the reaction rate of each catalysts at around 50–60% conversion of lauric acid at 170 °C, H_2 40 bar, after 180 min. We found that the reaction rate of lauric acid hydroconversion over Ru/TiO_2 (Ru = 5 wt%) was 3.40 mmol g_{cat}^{-1} min^{-1} (conversion 44%), while those over Ru–(0.011)MoO_x/TiO_2, Ru–(0.026)MoO_x/TiO_2, and Ru–(0.048)MoO_x/TiO_2 were 7.23 mmol g_{cat}^{-1} min^{-1} (conversion 76%), 9.43 mmol g_{cat}^{-1} min^{-1} (conversion 73%), 3.77 mmol g_{cat}^{-1} min^{-1} (conversion 58%), respectively. Therefore, it can be concluded that the optimum Mo loading amount in Ru–MoO_x/TiO_2 was 0.026 mmol (Mo/Ru = 0.5).

Effect of the temperature reduction. To get the insight into the role of MoO_x species during the reaction, the catalytic reactions using Ru–(0.026)MoO_x/TiO_2 catalyst was reduced with hydrogen different reduction temperatures, *ca.* 300 °C, 400 °C, 500 °C, and 600 °C (The XRD patterns of those catalysts are shown in Fig. S8, in the ESI†) and the results are shown in Fig. 2. By using Ru–(0.026)MoO_x/TiO_2 300 °C catalyst, the main product was dodecane-1-ol (58%) while *n*-dodecane and ester were 12% and 30%, respectively at complete reaction. When the catalyst was reduced at 400 °C, the yield of dodecane-1-ol reach to maximum (61%) while *n*-dodecane remarkably increased to 38%. Over this catalyst, the esterification reaction of lauric acid and dodecane-1-ol to formation dodecyl dodecanoate was inhibited as indicated by only small amount of ester (1%). Further increase the temperature reduction to 500 °C and 600 °C, yield of dodecyl dodecanoate slightly increased to 3% and 5%. However, the maximum yield of *n*-dodecane (44%) was obtained over Ru–(0.026)MoO_x/TiO_2 500 °C catalyst at full conversion of lauric acid. From these results, we fixed the catalytic hydroconversion of lauric acid with the Ru–(0.026)MoO_x/TiO_2 catalyst reduced at 400–500 °C as the most effective catalyst system.

Effect of reaction temperature. The influence of reaction temperature on the product distributions in the

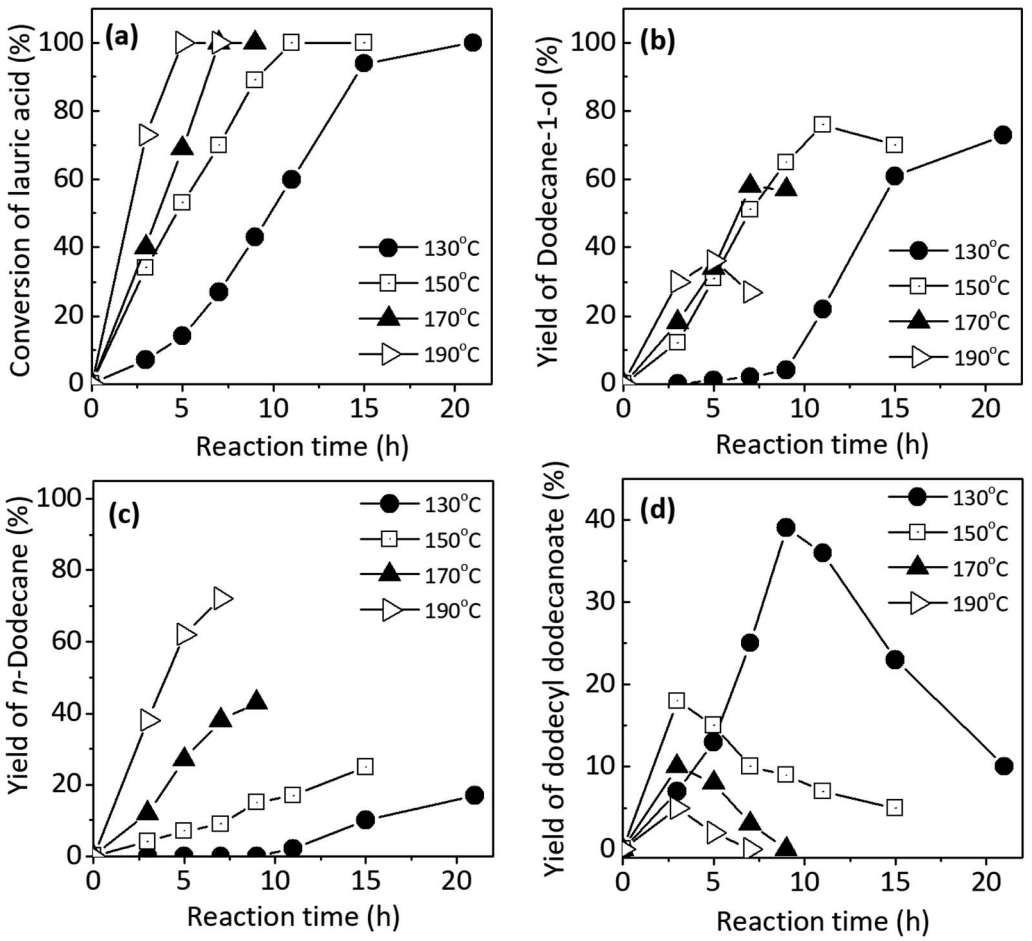

Fig. 5 (a) Time profiles of the hydroconversion of lauric acid; (b) yield of dodecane-1-ol as a function of time profiles of the hydroconversion of lauric acid; (c) yield of dodecane as a function of time profiles of the hydroconversion of lauric acid; and (d) yield of dodecyl dodecanoate as a function of time profiles of the hydroconversion of lauric acid over the Ru–(0.026)MoO_x/TiO_2 catalyst. Reaction conditions: catalyst, 0.065 g; lauric acid, 3.2 mmol; solvent, 2-propanol: H_2O, 5 ml (4.0 : 1.0 volume ratio); 130–190 °C, H_2 40 bar, 0–21 h.

Table 4 Results of selective hydroconversion of lauric acid and possible intermediates over Ru–(0.026)MoO_x/TiO_2 catalyst (Mo/Ru = 0.5)[a]

Entry	Substrate	Conversion[b] (%)	Yield[b] (%)			Rate of reactant reaction (r_R) (mmol g_{cat}^{-1} min^{-1})	Rate of product formation (r_P) (mmol g_{cat}^{-1} min^{-1})
			Dodecane-1-ol	*n*-Dodecane	Ester[c]		
1	Lauric acid	69	34	27	8	6.17	0.14
2	Methyl laurate	50	36	14	0	6.46	0.07
3	1-Dodecanal	67	37	30	0	9.17	0.27
4	Dodecane-1-ol	53	0	53	0	8.98	0.23
5	Dodecyl dodecanoate	7	0	5	0	0.91	0.02

[a] Reaction conditions: catalyst, 0.065 g; lauric acid, 3.2 mmol; solvent, 2-propanol: H_2O, 5.0 ml (4.0 : 1.0 volume ratio); H_2 40 bar; 170 °C, 3 h. [b] Conversion and yield were determined by GC using an internal standard technique. [c] Ester was dodecyl dodecanoate. The carbon balance was more than 96% for all the reactions.

hydroconversion of lauric acid over Ru–(0.026)MoO_x/TiO_2 catalyst is shown in Fig. 3.

The conversion of lauric acid increased gradually as the reaction temperature was increased from 130 °C and completed reaction (100% conversion) was achieved at 170 °C. The maximum yield of dodecane-1-ol was obtained at 150 °C then gradually decreased at 160 to 230 °C which is proportional with the increase of *n*-dodecane yield. The hydrodeoxygenation (*via* dehydration-hydrogenation) of lauric acid took place firstly to form dodecane-1-ol at lower temperature ≤150 °C and at the same time, the esterification of lauric acid and dodecane-1-ol to form dodecyl dodecanoate was also occurred at that of reaction temperature. At the reaction temperatures of 170–230 °C, the direct hydrodeoxygenation of lauric acid or subsequently take place the dehydration–hydrogenation reaction of formed dodecane-1-ol which are preferable occurred to yield *n*-dodecane. There no undecane product was observed, suggesting that decarbonylation/decarboxylation reaction did not proceed over the studied catalysts under current reaction conditions. Additionally, the esterification of lauric acid and formed dodecane-1-ol was also totally disappeared at that of the reaction temperatures. These results are good consistent with the report of Kon *et al.* who reported the hydrodeoxygenation of lauric acid using Pt–MoO_x/TiO_2 catalyst and produced dodecane (86% yield) at 100% conversion of lauric acid without the formation of dodecyl dodecanoate at 180 °C, 80 bar H_2 and 3 h.[13]

Effect of H_2 initial pressure. The influence of the initial H_2 pressure on the product distributions in the hydroconversion of lauric acid over Ru–(0.026)MoO_x/TiO_2 catalyst is shown in Fig. 4. The conversion of lauric acid increased as the initial H_2 pressure was increased to reach 100% conversion at 30 bar. The maximum yield *n*-dodecane (38%) were achieved at the initial H_2 pressure of 40 bar, while the yield of dodecyl dodecanoate decreased (≤3%). Therefore, it can be concluded that the effective hydroconversion of lauric acid to *n*-dodecane can be achieved at an initial H_2 pressure of 40 bar, was used as the optimised initial H_2 pressure for further investigations on the subsequent catalytic reactions for time profiles and the catalytic reaction of various carboxylic acids.

Time profiles. The kinetic profiles of the hydroconversion of lauric acid in the presence of Ru–(0.026)MoO_x/TiO_2 (Mo/Ru = 0.5) catalyst at 130–190 °C, initial H_2 pressure of 40 bar, and reaction times of 0–21 h were studied and the plots are shown in Fig. 5.

Fig. 5a shows the profile of lauric acid conversion as a function of reaction time at different reaction temperatures *ca.* 130 °C, 150 °C, 170 °C, and 190 °C. At 130 °C, the conversion of

Table 5 Results of selective hydroconversion of various fatty acids and carboxylic acid over Ru–(0.026)MoO_x/TiO_2 catalyst[a]

Entry	Substrate	Time (h)	Conversion[b] (%)	Main product	Selectivity[b] (%)	
					Alcohol	Alkanes
1	Octadecanoic acid (stearic acid)	15	92	Octadecanol	79	21
2	Hexadecanoic acid (palmitic acid)	9	83	Hexadecanol	80	20
3	Methyl palmitate	9	74	Hexadecanol	82	18
4	Tetradecanoic acid (myristic acid)	5	76	Tetradecanol	74	26
5	Dodecanoic acid (lauric acid)	7	>99	Dodecan-1-ol	61	39
6	Nonanoic acid	5	89	Nonanol	89	11
7	Octanoic acid	5	79	Octanol	87	13
8	Hexanoic acid	3	78	Hexanol	91	9
9[c]	Valeric acid	3	83	1-Pentanol	94	6
10[c]	Levulinic acid	3	>99	1,4-PeD(GVL)	81(19)	—
11[c]	Succinic acid	3	73	1,4-BeD(GBL)	63(37)	—

[a] Reaction conditions: catalyst, 0.065 g; lauric acid, 3.2 mmol; solvent, 2-propanol/H_2O, 5.0 ml (4.0 : 1.0 volume ratio); H_2 40 bar; 170 °C, 5–15 h. [b] Conversion and yield were determined by GC using an internal standard technique. [c] Reaction temperature was 110 °C. The carbon balance was more than 93–96% for all the reactions. 1,4-PeD = 1,4-Pentanediol. 1,4-BeD = 1,4-Butanediol. GVL = γ-Valerolactone. GBL = γ-Butyrolactone.

lauric acid increased smoothly as function of reaction time and the conversion achieved to 100% after 20 h. At 150 °C, the completed reaction was achieved after 10 h indicating that the conversion of lauric acid took place faster (approximately two times) than that of 130 °C. As the reaction temperatures were increased to 170 °C and 190 °C, the reaction rate of lauric acid conversion become faster as indicated by the completed reaction after 7 h and 5 h, respectively.

Fig. 5b displays the profile of dodecane-1-ol yield as function of reaction time at different temperatures. At 130 °C, the formation of dodecane-1-ol was observed firstly after 7 h, then increased gradually to reach maximum yield of 73% at 100% conversion lauric acid after 21 h. The highest yield of dodecane-1-ol (75%) was obtained at reaction temperature of 150 °C after 11 h and the amount of dodecane-1-ol slightly decreased to 70% when the reaction time was prolonged to 15 h. The decrease of dodecane-1-ol yield can be attributed to due to the further reaction of dodecane-1-ol (*via* dehydration/hydrogenation) to *n*-dodecane or esterification with lauric acid to form dodecyl dodecanoate. Kon *et al.* suggested that the esterification between dodecane-1-ol and lauric acid (dodecanoate) gave dodecyl dodecanoate in the presence of Pt/Nb_2O_5 or $Rh–MoO_x/TiO_2$ catalysts at 180 °C.[13] However, in our Ru–(0.026)MoO_x/TiO_2 catalyst, the significant formation of dodecyl dodecanoate is favourable occurred at reaction temperature of ≤150 °C (Fig. 3) or at low initial H_2 pressure (Fig. 4). The yield of dodecyl dodecanoate (Fig. 5c) increased to reach maximum yield of 39% at reaction temperature 130 °C after 9 h, then getting decrease as reaction time was prolonged up to 21 h. On the other hand, the amount of ester product not more than 18% when the reaction temperature increased to 150–190 °C, suggesting that further hydrogenation of ester was favourable occurred at high reaction rate. Results of catalytic performance of various $Ru–MoO_x$ catalysts confirm that the amount of remained ester product <0.1 and 0 at the reaction temperature of 170 °C and 190 °C, respectively. Moreover, the profiles of *n*-dodecane yield (Fig. 5d) also confirmed that the proposed reaction pathway in Scheme 1 is basically consistent with those for the hydrodeoxygenation of fatty acids by Pt/Nb_2O_5[74] and $Pt–MoO_x/TiO_2$[13] catalysts.

Table 4 compares the results for hydrogenation of possible intermediates (methyl laurate, dodecanal, dodecane-1-ol, dodecyl dodecanoate) and lauric acid under the same reaction conditions. We obtained that the reaction rate of oxygenate conversion changed in the following order: 1-dodecanal (9.17 mmol g_{cat}^{-1} min^{-1}) > dodecane-1-ol (9.17 mmol g_{cat}^{-1} min^{-1}) > methyl laurate (6.46 mmol g_{cat}^{-1} min^{-1}) ≈ lauric acid (6.17 mmol g_{cat}^{-1} min^{-1})> >> dodecyl dodecanoate (0.91 mmol g_{cat}^{-1} min^{-1}). Lauric acid showed highest conversion to produce 34% yield of dodecane-1-ol, 27% yield *n*-dodecane and 8% ester (dodecyl dodecanoate (entry 1). The formation of ester both in alcoholic or 2-propanol/H_2 mixture solvents took place faster than that of *n*-dodecane as indicated by the high yield of ester (Table 1, entries 1–3) and (Table 4, entry 1). Notably, lauric acid underwent esterification with dodecane-1-ol at low reaction temperature (Fig. 3) or in low initial H_2 pressure (Fig. 4). Dodecane-1-ol can also undergo esterification with lauric acid to give dodecyl dodecanoate, which is then hydrogenated to *n*-dodecane *via* dodecane-1-ol. Therefore, it can concluded that the hydroconversion of lauric acid in the presence of $Ru–(y)MoO_x/TiO_2$ catalysts follows the proposed reaction pathway as shown in Scheme 1.

Hydroconversion of various fatty acids. The scope of the hydroconversion using $Ru–(0.026)MoO_x/TiO_2$ catalyst was further extended to various other aliphatic carboxylic acids and the results are summarised in Table 5. In all cases, high activity at low reaction temperatures was found with similar reaction rate. Catalytic hydroconversion of higher carbon number aliphatic carboxylic acids (C ≥ 12) (entries 1–5) resulted higher selectivity towards alkanes than that of lower carbon number (C5–C9) (entries 6–9). Moreover, $Ru–(0.026)MoO_x/TiO_2$ catalyst was also active for hydroconversion of typical biomass-derived dicarboxylic acids (*e.g.*, levulinic acid and succinic acid) produced diols and lactone under mild reaction conditions (entries 10–11).

The reusability of $Ru–(0.026)MoO_x/TiO_2$ catalyst was studied with the recovered catalyst regenerated by washing with acetone following by pre-reduction in H_2 at 400 °C for 2 h and then the hydroconversion of lauric acid repeated. The regenerated $Ru–(0.026)MoO_x/TiO_2$ catalyst showed loss in the hydrogenation activity with an associated in reaction rate. A further loss in the hydrogenation activity was observed on recycling the catalyst for a second time. Some of the decrease in activity is likely to be due to aggregation of active metal during the reaction or the collaps of catalyst structures (XRD patterns and TEM images of recovered $Ru–(0.026)MoO_x/TiO_2$ catalyst are shown in Fig. S9 and S10, in the ESI†).

Experimental

Catalyst preparation

A typical procedure for the synthesis of $Ru–(0.026)MoO_x/TiO_2$ (0.026 is Mo loading amount Mo) described as follows:[75] $RuCl_3$ (0.049 mmol) was dissolved in deionized water (denoted as solution A) and $(NH_4)_6Mo_7O_{24}\cdot 4H_2O$ (0.026 mmol) was dissolved in ethanol/ethylene glycol (2.0/1.0 volume ratio) (denoted as solution B) at room temperature. Solutions A, B, and TiO_2 (as support material; 1.0 g) were mixed at room temperature; the temperature was subsequently raised to 50 °C under gentle stirring for 12 h. The pH of the mixture was adjusted to 12 through the dropwise addition of an aqueous solution of NaOH (3.1 M). The mixture was then placed into a sealed-Teflon autoclave for the hydrothermal process at 150 °C for 24 h. The resulting black precipitate was filtered, washed with distilled water, and then dried under vacuum overnight. Prior to the catalytic reaction, the obtained black powder was treated under hydrogen at 500 °C for 3 h.

Catalyst characterization

The X-ray diffraction (XRD) analysis was performed on a Miniflex 600 Rigaku instrument with Cu as monochromatic source of Cu$K\alpha$ radiation (λ = 0.15444 nm). The XRD was operated at 40 kV and 15 mA with a step width of 0.02°, a scan speed of 4° min^{-1} (α_1 = 0.154 057 nm, α_2 = 0.154 433 nm), solar slit 1.25°, and using a Ni $K\beta$ filter. ICP measurements were

performed on an SPS 1800H plasma spectrometer by Seiko Instruments Inc. Japan (Ni: 221.7162 nm and Sn: 189.898 nm).

The BET surface area (S_{BET}) and pore volume (V_p) were measured using N_2 physisorption at −196 °C on a Belsorp Max (BEL Japan). The samples were degassed at 200 °C for 2 h to remove physisorbed gases prior to the measurement. The amount of nitrogen adsorbed onto the samples was used to calculate the Brunauer–Emmett–Teller (BET) surface area *via* the BET equation. The pore volume was estimated to be the liquid volume of nitrogen at a relative pressure of approximately 0.995 according to the Barrett–Joyner–Halenda (BJH) approach based on desorption data.[76]

The NH_3–TPD was carried out on a Belsorp Max (BEL Japan). The samples were degassed at elevated temperature of 100–200 °C for 2 h to remove physisorbed gases prior to the measurement. The temperature was then kept at 200 °C for 2 h while flushed with He gas. NH_3 gas (balanced NH_3, 80% and He, 20%) was introduced at 100 °C for 30 min, then evacuated by helium gas to remove the physisorbed also for 30 min. Finally, temperature programmed desorption was carried out at temperature of 100–800 °C and the desorbed NH_3 was monitored by TCD. SEM images of the synthesised catalysts were taken on a JEOL JSM-610 SEM after the samples were coated using a JEOL JTC-1600 auto fine coater. The TEM images were taken on Hitachi H7650 at 19 kV.

The H_2 uptake was determined through irreversible H_2 chemisorption. After the catalyst was heated at 100 °C under vacuum for 30 min, it was heated at 400 °C under H_2 for 30 min. The catalysts were subsequently cooled to room temperature under vacuum for 30 min. The H_2 measurement was conducted at 0 °C, and H_2 uptake was calculated according to the method described in the literature.[77]

Catalytic reaction

Lauric acid hydroconversion. Typical procedure for hydrogenation of lauric acid describes as follows: catalysts (0.05 g), lauric acid (3.2 mmol), decalin (0.02 mmol), and *iso*-propanol/H_2O (5.0 ml; 4.0/1.0 volume ratio) as solvent were placed into a glass reaction tube in an autoclave reactor system of TAIATSU Techno reactor a Pyrex tube was fitted inside of a sus316 jacket to protect the vessel from corrosion in acidic media. The reactor was flushed with 1.0 bar H_2 for 10 times to remove undesired gas prior to the reaction. After H_2 was introduced into the reactor with an initial H_2 pressure of 40 bar at room temperature, the temperature of the reactor was increased to 170 °C under constant stirring (800 rpm). After 7 h, the conversion of lauric acid and the yield of lauryl alcohol were determined by gas chromatography (GC) analysis.

Product analysis. Gas chromatography analysis of the reactant (dodecanoic acid) and products was performed on a PerkinElmer Autosystem XL with a flame ionization detector with an InertCap 225 (i.d. 0.25 mm, length 30 m, d.f. 0.25 mm) capillary column of GL Science Inc. Tokyo Japan. The products were confirmed by a comparison of their GC retention time, mass spectra with those of authentic samples. Gas chromatography–mass spectrometry (GC-MS) was performed on a Shimadzu GC-17B equipped with a thermal conductivity detector and an RT-βDEXsm capillary column.

The calibration curve was performed using known concentrations of internal standard, reactants and products in order to determine the correct response factors. The conversion of dodecanoic acid, yield and selectivity of the products were calculated according to the following equations:

$$\text{Conversion}: \frac{\text{Introduced mol reactant}(C_0) - \text{Remained mol reactant}(C_t)}{\text{Introduced mol reactant}(C_0)} \times 100\%$$

$$\text{Yield}: \frac{\text{Mol product}}{\text{Introduced mol reactant}(C_0)} \times 100\%$$

where C_o is the introduced mol reactant (dodecanoic acid), C_t is the remaining mol reactant, and ΔC is the consumed mol reactant (introduced mol reactant – remained mol reactant), which are all obtained from GC analysis using an internal standard technique.

The apparent reaction rates were calculated using the following equation:

$$r_{\text{lauric acid}} = \frac{W}{mt} \times x_{\text{lauric acid}}$$

where $r_{\text{Lauric acid}}$ is the apparent reaction rate of lauric acid (mol g_{cat}^{-1} min^{-1}), W is the molar weight of the reactant (mol), t is the reaction duration (s), $x_{\text{Lauric acid}}$ is the conversion of stearic acid (%), and m is the catalyst weight (g).

The formation rates of the products were calculated using the following equation:

$$r_{\text{product}} = \frac{W}{mt} \times x_{\text{lauric acid}} \times S_{\text{product}}$$

where $r_{\text{Lauric acid}}$ is the apparent reaction rate of lauric acid (mol g_{cat}^{-1} min^{-1}), W is the molar weight of the reactant (mol), t is the reaction duration (s), $x_{\text{Lauric acid}}$ is the conversion of stearic acid (%), s_{Product} is the selectivity of the product, and m is the catalyst weight (g).

Conclusions

We described the selective hydroconversion of coconut oil derived lauric acid to lauryl alcohol and *n*-dodecane in 2-propanol/water (4.0/1.0 v/v) mixture solvent using molybdenum oxide-modified ruthenium on titanium oxide (Ru–(y)MoO_x/TiO_2; y = Mo loading amount, mmol g^{-1}) catalysts. Among the Ru–(y)MoO_x/TiO_2 catalysts tested, Ru–(0.026)MoO_x/TiO_2 (Mo loading amount of 0.026 mmol g^{-1}) shows the highest yields of *n*-alkanes for hydroconversion of coconut oil derived lauric acid and hydroconversion of various aliphatic fatty acids C8–C18 precursor at 170–230 °C, 30–40 bars for 7–20 h. At lower reaction temperatures ($130 \geq T \leq 150$ °C), the main product was dodecane-1-ol and dodecyl dodecanoate as the results of hydrogenation of lauric acid and esterification of lauric acid

and corresponding alcohols. The presence of MoO_x/TiO_2 might played as Lewis acid sites which cooperated with Ru nanoparticles as H_2 dissociation sites, led to high activity of Ru–(y) MoO_x/TiO_2 catalysts, and suppressed the $HDCO_2$ or HDCO reactions, thus produced high aliphatic alcohols and aliphatic alkanes with same carbon number. Over the Ru–(0.026)MoO_x/TiO_2 as the best catalyst, an increase in reaction temperature up to 230 °C significantly enhanced the degree of hydrodeoxygenation of lauric acid and produced *n*-dodecane with maximum yield (up to 80%) at 230 °C, H_2 40 bar for 7 h. Ru–(0.026)MoO_x/TiO_2 is also effective for the hydroconversion of various dicarboxylic acids to the corresponding lactones and diols.

Author contributions

Rodiansono: conceptualization, methodology, investigation, writing – original draft, writing – review & editing. Heny Puspita Dewi, Kamilia Mustikasari, Maria Dewi Astuti, Sadang Husain, and Sutomo: formal analysis, investigation, and visualization.

Conflicts of interest

The authors declare that they have no known competing financial interests or personal relationships that could have appeared to influence the work reported in this paper.

Acknowledgements

The authors acknowledge the RISET DASAR FY 2019–2021 (contract number DIPA-042.06-1.401516/2020) and RISET DASAR FY 2021–2023 (119/E4.1/AK.04.PT/2021) from Ministry of Education, Culture, Research and Technology, Indonesian Government for financially supported this work. These works were partially supported by BPDP-Sawit, Ministry of Finances through GRK-2016 under contract number PRJ-49/2016.

Notes and references

1 N. Hongloi, P. Prapainainar and C. Prapainainar, *Mol. Catal.*, 2021, 111696.
2 X. Yao, T. J. Strathmann, Y. Li, L. E. Cronmiller, H. Ma and J. Zhang, *Green Chem.*, 2021, **23**, 1114–1129.
3 H. I. Mahdi, A. Bazargan, G. McKay, N. I. W. Azelee and L. Meili, *Chem. Eng. Res. Des.*, 2021, **174**, 158–187.
4 M. A. Sánchez, G. C. Torres, V. A. Mazzieri and C. L. Pieck, *J. Chem. Technol. Biotechnol.*, 2017, **92**, 27–42.
5 U. Biermann, U. Bornscheuer, M. A. R. Meier, J. O. Metzger and H. J. Schäfer, *Angew. Chem., Int. Ed.*, 2011, **50**, 3854–3871.
6 K. Noweck and W. Grafahrend, in *Ullmann's Encyclopedia of Industrial Chemistry*, Wiley-VCH Verlag GmbH & Co. KGaA, Weinheim, Germany, 2006, vol. 14, pp. 117–141.
7 S. Lestari, P. Mäki-Arvela, J. Beltramini, G. Q. M. Lu and D. Y. Murzin, *ChemSusChem*, 2009, **2**, 1109–1119.
8 M. W. Schreiber, D. Rodriguez-Niño, O. Y. Gutiérrez and J. A. Lercher, *Catal.: Sci. Technol.*, 2016, **6**, 7976–7984.
9 G. J. S. Dawes, E. L. Scott, J. Le Nôtre, J. P. M. Sanders and J. H. Bitter, *Green Chem.*, 2015, **17**, 3231–3250.
10 K. C. Sembiring and S. Saka, *J. Jpn. Pet. Inst.*, 2019, **62**, 157–172.
11 M. Tamura, Y. Nakagawa and K. Tomishige, *Asian J. Org. Chem.*, 2020, **9**, 126–143.
12 M. Mohammad, T. Kandaramath Hari, Z. Yaakob, Y. Chandra Sharma and K. Sopian, *Renewable Sustainable Energy Rev.*, 2013, **22**, 121–132.
13 K. Kon, T. Toyao, W. Onodera, S. M. A. H. Siddiki and K. I. Shimizu, *ChemCatChem*, 2017, **9**, 2822–2827.
14 Ł. J□czmionek and K. Porzycka-Semczuk, *Fuel*, 2014, **131**, 1–5.
15 S. Kim, E. E. Kwon, Y. T. Kim, S. Jung, H. J. Kim, G. W. Huber and J. Lee, *Green Chem.*, 2019, **21**, 3715–3743.
16 D. M. Alonso, S. G. Wettstein and J. A. Dumesic, *Chem. Soc. Rev.*, 2012, **41**, 8075–8098.
17 J. Pritchard, G. A. Filonenko, R. Van Putten, E. J. M. Hensen and E. A. Pidko, *Chem. Soc. Rev.*, 2015, **44**, 3808–3833.
18 M. Besson, P. Gallezot and C. Pinel, *Chem. Rev.*, 2014, **114**, 1827–1870.
19 P. Mäki-Arvela, M. Snåre, K. Eränen, J. Myllyoja and D. Y. Murzin, *Fuel*, 2008, **87**, 3543–3549.
20 J. Zhang, X. Huo, Y. Li and T. J. Strathmann, *ACS Sustainable Chem. Eng.*, 2019, **7**, 14400–14410.
21 J. Wu, J. Shi, J. Fu, J. A. Leidl, Z. Hou and X. Lu, *Sci. Rep.*, 2016, **6**, 1–8.
22 L. Yang, K. L. Tate, J. B. Jasinski and M. A. Carreon, *ACS Catal.*, 2015, **5**, 6497–6502.
23 I. Simakova, O. Simakova, P. Mäki-Arvela and D. Y. Murzin, *Catal. Today*, 2010, **150**, 28–31.
24 N. Chen, Y. Ren and E. W. Qian, *J. Catal.*, 2016, **334**, 79–88.
25 R. Rodiansono, M. I. Pratama, M. D. Astuti, A. Abdullah, A. Nugroho and S. Susi, *Bull. Chem. React. Eng. Catal.*, 2018, **13**, 311–319.
26 K. Kon, W. Onodera, S. Takakusagi and K. I. Shimizu, *Catal.: Sci. Technol.*, 2014, **4**, 3705–3712.
27 F. Liu, J. Ftouni, P. C. A. Bruijnincx and B. M. Weckhuysen, *ChemCatChem*, 2019, **11**, 2079–2088.
28 X. Cao, F. Long, Q. Zhai, J. Zhao, J. Xu and J. Jiang, *Fuel*, 2021, **298**, 120829.
29 K. Tomishige, Y. Nakagawa and M. Tamura, *Green Chem.*, 2017, **19**, 2876–2924.
30 V. M. Deshpande, K. Ramnarayan and C. S. Narasimhan, *J. Catal.*, 1990, **182**, 174–182.
31 T. Miyake, T. Makino, S. ichi Taniguchi, H. Watanuki, T. Niki, S. Shimizu, Y. Kojima and M. Sano, *Appl. Catal., A*, 2009, **364**, 108–112.
32 V. M. Deshpande, W. R. Patterson and C. S. Narasimhan, *J. Catal.*, 1990, **121**, 165–173.
33 C. Huang, H. Zhang, Y. Zhao, S. Chen and Z. Liu, *J. Colloid Interface Sci.*, 2012, **386**, 60–65.
34 R. Rodiansono, M. I. Pratama, M. D. Astuti, A. Abdullah, A. Nugroho and S. Susi, *Bull. Chem. React. Eng. Catal.*, 2018, **13**, 311–319.
35 Y. Shao, Q. Xia, X. Liu, G. Lu and Y. Wang, *ChemSusChem*, 2015, **8**, 1761–1767.

36 R. Rodiansono, E. Hayati, A. S. Azzahra, M. D. Astuti, K. Mustikasari, S. Husain and S. Sutomo, *Bull. Chem. React. Eng. Catal.*, 2021, **16**, 888–903.

37 Z. Luo, Q. Bing, J. Kong, J. Y. Liu and C. Zhao, *Catal.: Sci. Technol.*, 2018, **8**, 1322–1332.

38 M. J. Hidajat, G. N. Yun and D. W. Hwang, *Mol. Catal.*, 2021, **512**, 111770.

39 S. Liu, W. Zheng, J. Fu, K. Alexopoulos, B. Saha and D. G. Vlachos, *ACS Catal.*, 2019, **9**, 7679–7689.

40 T. Asano, Y. Nakagawa, M. Tamura and K. Tomishige, *ACS Sustainable Chem. Eng.*, 2019, **7**, 9601–9612.

41 T. Arai, M. Tamura, Y. Nakagawa and K. Tomishige, *ChemSusChem*, 2016, **9**, 1680–1688.

42 Y. Takeda, T. Shoji, H. Watanabe, M. Tamura, Y. Nakagawa, K. Okumura and K. Tomishige, *ChemSusChem*, 2015, **8**, 1170–1178.

43 T. Asano, M. Tamura, Y. Nakagawa and K. Tomishige, *ACS Sustainable Chem. Eng.*, 2016, **4**, 6253–6257.

44 Y. Cao, H. Zhang, K. Liu, Q. Zhang and K. J. Chen, *ACS Sustainable Chem. Eng.*, 2019, **7**, 12858–12866.

45 Y. Yang, Q. Liu, D. Li, J. Tan, Q. Zhang, C. Wang and L. Ma, *RSC Adv.*, 2017, **7**, 16311–16318.

46 Y. Zheng, Z. Tang and S. G. Podkolzin, *Chem.–Eur. J.*, 2020, **26**, 5174–5179.

47 S. Liu, W. Zheng, J. Fu, K. Alexopoulos, B. Saha and D. G. Vlachos, *ACS Catal.*, 2019, **9**, 7679–7689.

48 S. Koso, H. Watanabe, K. Okumura, Y. Nakagawa and K. Tomishige, *Appl. Catal., B*, 2012, **111–112**, 27–37.

49 K. I. Shimizu, S. Kanno and K. Kon, *Green Chem.*, 2014, **16**, 3899–3903.

50 J. Guan, G. Peng, Q. Cao and X. Mu, *J. Phys. Chem. C*, 2014, **118**, 25555–25566.

51 K. Tomishige, Y. Nakagawa and M. Tamura, *Curr. Opin. Green Sustainable Chem.*, 2020, **22**, 13–21.

52 J. A. Bezard, *Lipids*, 1971, **6**, 630–634.

53 J. Bezard, M. Bugaut and G. Clement, *J. Am. Oil Chem. Soc.*, 1971, **48**, 134–139.

54 R. Rodiansono, M. D. Astuti, T. Hara, N. Ichikuni and S. Shimazu, *Catal. Sci. Technol.*, 2016, **6**, 2955–2961.

55 R. Rodiansono, M. D. Astuti, A. Ghofur and K. C. Sembiring, *Bull. Chem. React. Eng. Catal.*, 2015, **10**, 192–200.

56 A. P. Damayanti, H. P. Dewi, I. Ibrahim and R. Rodiansono, in *IOP Conference Series: Materials Science and Engineering*, 2020, vol. 980, p. 012013.

57 I. Ibrahim, M. Riski and R. Rodiansono, in *IOP Conference Series: Materials Science and Engineering*, 2020, vol. 980, p. 012012.

58 D. R. Vardon, B. K. Sharma, H. Jaramillo, D. Kim, J. K. Choe, P. N. Ciesielski and T. J. Strathmann, *Green Chem.*, 2014, **16**, 1507–1520.

59 J. Zhang, X. Huo, Y. Li and T. J. Strathmann, *ACS Sustainable Chem. Eng.*, 2019, **7**, 14400–14410.

60 J. Fu, X. Lu and P. E. Savage, *ChemSusChem*, 2011, **4**, 481–486.

61 E. A. Cepeda, R. Bravo and B. Calvo, *J. Chem. Eng. Data*, 2009, **54**, 1371–1374.

62 K. Yui, Y. Itsukaichi, T. Kobayashi, T. Tsuji, K. Fukui, K. Maeda and H. Kuramochi, *J. Chem. Eng. Data*, 2017, **62**, 35–43.

63 A. B. Gonçalves Bonassoli, G. Oliveira, F. H. Bordón Sosa, M. P. Rolemberg, M. A. Mota, R. C. Basso, L. Igarashi-Mafra and M. R. Mafra, *J. Chem. Eng. Data*, 2019, **64**, 2084–2092.

64 M. A. Mellmer, C. Sener, J. M. R. Gallo, J. S. Luterbacher, D. M. Alonso and J. A. Dumesic, *Angew. Chem., Int. Ed.*, 2014, **53**, 11872–11875.

65 M. A. Mellmer, C. Sener, J. M. R. Gallo, J. S. Luterbacher, D. M. Alonso and J. A. Dumesic, *Angew. Chem.*, 2014, **126**, 12066–12069.

66 T. Asano, Y. Nakagawa, M. Tamura and K. Tomishige, *ACS Sustainable Chem. Eng.*, 2019, **7**, 9601–9612.

67 H. G. Manyar, C. Paun, R. Pilus, D. W. Rooney, J. M. Thompson and C. Hardacre, *Chem. Commun.*, 2010, **46**, 6279–6281.

68 T. Mizugaki, Y. Nagatsu, K. Togo, Z. Maeno, T. Mitsudome, K. Jitsukawa and K. Kaneda, *Green Chem.*, 2015, **17**, 5136–5139.

69 J. Cui, J. Tan, Y. Zhu and F. Cheng, *ChemSusChem*, 2018, **11**, 1316–1320.

70 T. Toyao, S. Kayamori, Z. Maeno, S. M. A. H. Siddiki and K. Shimizu, *ACS Catal.*, 2019, **9**, 8187–8196.

71 Y. Takeda, T. Shoji, H. Watanabe, M. Tamura, Y. Nakagawa, K. Okumura and K. Tomishige, *ChemSusChem*, 2015, **8**, 1170–1178.

72 H. P. Dewi, J. Santoso, N. F. Trianda and R. Rodiansono, *J. Kim. Sains Apl.*, 2019, **22**, 299–304.

73 K. Putri, A. Annisa, S. Husain and R. Rodiansono, *Bull. Chem. React. Eng. Catal.*, 2020, **15**, 35–42.

74 K. Kon, W. Onodera, S. Takakusagi and K. I. Shimizu, *Catal.: Sci. Technol.*, 2014, **4**, 3705–3712.

75 R. Rodiansono, S. Khairi, T. Hara, N. Ichikuni and S. Shimazu, *Catal.: Sci. Technol.*, 2012, **2**, 2139–2145.

76 S. Lowell, J. E. Shields, M. A. Thomas and M. Thommes, *Characterization of Porous Solids and Powders: Surface Area, Pore Size and Density*, Springer Netherlands, Dordrecht, 2004, vol. 16.

77 C. H. Bartholomew and R. B. Pannell, *J. Catal.*, 1980, **65**, 390–401.